

CERTIFICATE

This is to certify that the thesis entitled “**Design and Simulation Investigations of Single/Dual Frequency Relativistic Backward Wave Oscillators**” being submitted by **V Venkata Reddy (17091028)**, to the Indian Institute of Technology (Banaras Hindu University), Varanasi, for the award of the Degree of Doctor of Philosophy in the Department of Electronics Engineering is a record of bonafide research work carried out absolutely by him under my supervision and guidance. The thesis has reached the standard; fulfilling the requirements of the regulations relating to the nature of degree. The results embodied in this thesis have not been submitted to any other university or institute for the award of any degree or diploma.


(Dr. M. Thottappan)

Supervisor


19.07.22

(Prof. V. N. Mishra)

आचार्य/Head of the Department OR & HEAD
एलेक्ट्रॉनिक्स अभियांत्रिकी विभाग/Department of Electronics Engineering
भारतीय प्रौद्योगिकी संस्थान (का हि वि)/Indian Institute of Technology (IIT) BHU
वाराणसी/Varanasi-221005 (INDIA) 19/8

CANDIDATE DECLARATION

I, **V Venkata Reddy**, certify that the work embodied in this thesis is my own bonafide work and carried out by me under the supervision of Dr. M. Thottappan from **25/07/2017** to **19/07/2022**, at the Department of Electronics Engineering, Indian Institute of Technology (Banaras Hindu University), Varanasi. The matter embodied in this thesis has not been submitted for the award of any other degree/diploma. I declare that I have faithfully acknowledged and given credits to the research workers wherever their works have been cited in my work in this thesis. I further declare that I have not willfully copied any other's work, paragraphs, text, data, results, etc., reported in journals, books, magazines, reports, dissertations, theses, etc., or available at websites and have not included them in this thesis and have not cited as my own work.

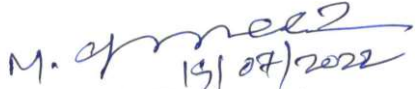
Date: 19/07/2022
Place: IIT (BHU), Varanasi


(V Venkata Reddy)

CERTIFICATE BY THE SUPERVISOR

It is certified that the above statement made by the student is correct to the best of my knowledge.

Date: 19/07/2022
Place: IIT (BHU), Varanasi


(Dr. M. Thottappan)
Supervisor


Signature of Head of Department

"SEAL OF THE DEPARTMENT"

इलेक्ट्रॉनिकी अभियांत्रिकी विभाग/Department of Electronics Engineering

भारतीय प्रौद्योगिकी संस्थान (का.हि.वि.)/Indian Institute of Technology (IIT)

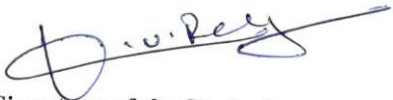
v वाराणसी/Varanasi-221005


19/7

Copyright Transfer

The undersigned hereby assigns to the Indian Institute of Technology (Banaras Hindu University), Varanasi all rights under copyright that may exist in and for the above thesis submitted for the award of the Doctor of Philosophy.

Date: 19/07/2022
Place: IIT (BHU), Varanasi


Signature of the Student
V Venkata Reddy

Note: However, the author may reproduce or authorize others to reproduce material extracted verbatim from the thesis or derivative of the thesis for author's personal use provided that the source and the Institute's copyright notice are indicated.

ACKNOWLEDGEMENTS

I express my immense gratitude to my supervisor Dr. M. Thottappan, for his excellent guidance and motivation. The completion of this research work is indeed an outcome of his constant tireless support, valuable ideas, and suggestions during my research work. The insightful discussions with him always provided me with great enthusiasm.

I wish to extend my sincere gratitude towards my research performance evaluation committee (RPEC) members, Prof. Sanjay Kumar Singh, and Dr. Smrity Dwivedi, for their encouragement and insightful comments. I would also like to thank all the faculty members, especially to Dr. Somak Bhattacharyya for their kind cooperation and encouragement during this journey.

I would like to express my special thanks to Dr. Anshu Sharan Singh, and Dr. V. Siva Venkateswara Rao for their valuable assistance at my initial stage of research work.

I am thankful to my colleagues Dr. Mumtaz A. Ansari, Mr. Shyam Gopal Yadav, Mr. Gundu Venkatesh, Mr. V Veera Babu, Mr. Vijay Kumar Devarakonda, and Mr. M Hemanta Kumar for their personal and technical support. I am very much thankful to many research scholars of the CRMT laboratory for providing a stimulating and friendly environment. My thanks go to Dr. Rajan Agrahari, Dr. Akash, Dr. Rajanish Kumar Singh, Dr. Vineet Singh, Dr. Prabhakar Tripathi, Mr. Vikram Rawat, Dr. Soumojit Shee. Mr. Sambit Ghosh, Mr. Diptiranjana Samantaray, Mr. Nilotpal, Mr. Nishith Mr. Ashutosh Kumar Dikshit, and Ms. Pratibha Verma.

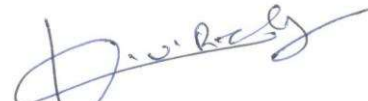
I would like to thank my friends and colleagues Dr. Pelluri Sambaiah, Mr. Ravishankar Simhadri, Dr. P Venkatappa Reddy, Mr. G.S.R Satyanarayana, Mr. M Siva Srinivasa Rao, Mr. G Surya Chand, Mr. Katta Ashok Kumar, Mr. N Srikanta, Dr. N Usha Rani, and Dr. T Pitchaiah, who not only gave me a professional look but also inspired me socially and emotionally.

I am thankful to the AICTE, GoI, New Delhi and Vignan's Foundation for Science, Technology & Research (Deemed to be University), Vadlamudi, Guntur for the financial assistantship during Ph.D. through the QIP-AICTE fellowship.

Finally, I heartily express sincere thanks to my family. For their unconditional love, extreme patience, and constant support over the years. They provide me strength and confidence to attain this task.

Above all, I bow my head before almighty Lord Venkateswara and Lord Vishwanath for providing me the strength and courage in completing my research work.

Date: 19/07/2022



(V Venkata Reddy)

Dedicated
To
My Family

CONTENTS

<i>List of Figures</i>	<i>xix</i>
<i>List of Tables</i>	<i>xxv</i>
<i>List of Abbreviations</i>	<i>xxvii</i>
<i>List of symbols</i>	<i>xxxi</i>
<i>Preface</i>	<i>xxxv</i>
CHAPTER 1: INTRODUCTION AND LITERATURE REVIEW.....	1
1.1 Introduction	1
1.2 Overview of High-Power Microwave Sources	3
1.2.1 Prime Power Supply	5
1.2.2 Pulse Power Supply	5
1.2.3 HPM Sources.....	7
1.2.4 Mode Convertor.....	8
1.2.5 Antenna.....	9
1.3 Overview of different HPM Sources.....	10
1.3.1 Relativistic Klystron Amplifier	12
1.3.2 Relativistic Magnetron	14
1.3.3 Virtual Cathode Oscillators (VCO or Vircator)	16
1.3.4 Magnetically Insulated Line Oscillator (MILO)	17
1.3.5 Reltron	20
1.3.6 Free Electron Laser.....	22
1.3.7 Relativistic Gyrotron Devices	23
1.4 Relativistic Backward Wave Oscillator (RBWO).....	24
1.4.1 Advantages of an RBWO	26
1.4.2 Applications of an RBWO.....	27
1.5 Literature Review of an RBWO.....	29
1.6 Problem Definition.....	34
1.7 Outline of the Thesis	35
1.8 Conclusion.....	39
CHAPTER 2: DESIGN INVESTIGATIONS AND PIC SIMULATION OF SIBGLE FREQUENCY RELATIVISTIC BACKWARD WAVE OSCILLATOR.....	43
2.1 Introduction	43
2.2 Operating Principle and Condition for Sustained Oscillation.....	45

2.3 Modeling of Sub-Assemblies	48
2.3.1 Annular Cathode	49
2.3.2 Reflector.....	50
2.3.3 Slow Wave Structure (SWS)	55
2.3.4 Tapered Waveguide Collector	57
2.3.5 Guiding Magnetic Field	58
2.4 Analytical Background of Relativistic BWO	589
2.4.1 Beam Power of thin annular electron beam.....	59
2.4.2 Dispersion Relation Sinusoidally Corrugated SWS	62
2.5 Simulation Results and Discussion.....	65
2.5.1 Cold Simulation	67
2.5.2 Particle-In-Cell (PIC) Simulation	68
2.6 Parametric Analysis and Discussion.....	70
2.6.1 Beam Voltage (V_b)	70
2.6.2 Corrugation Amplitude (r_0).....	71
2.6.3 Drift Length (L_{dr})	72
2.6.4 Magnetic Field (B)	73
2.7 Conclusion	74
CHAPTER 3: MODELLING OF RF PULSE SHORTENING CAUSES AND THEIR EFFECTS	
ON RBWO UNDER LOW GUIDING MAGNETIC FIELD	79
3.1 Introduction	79
3.2 Overview of Simulation Techniques in VED's.....	80
3.3 Design and Simulation of Non-Overmoded RBWO with RR.....	82
3.4 Simulation Study of RF Pulse Shortening.....	87
3.4.1 Modeling of various causes of RF pulse shortening.....	87
3.4.2 Simulation Study of Combined Causes of RF Pulse Shortening and their effects in RBWO Operation.....	92
3.5 Conclusion.....	98
CHAPTER 4: DESIGN AND SIMULATION INVESTIGATIONS OF S-BAND RBWO WITH	
SECTIONAL BRAGG REFLECTOR.....	103
4.1 Introduction	103
4.2 Bragg Reflector.....	105
4.2.1 Design Methodology.....	105
4.2.2 Coupling Coefficient and Power Reflection/Conversion Coefficient	1077

4.2.3 Cold analysis of Sectional BRAGG Structure.....	108
4.3 Slow Wave Structure (SWS).....	109
4.4 Modelling of PIC Simulation Results	110
4.5 Parametric Analysis	114
4.5.1 Effect on frequency and RF power with magnetic field.....	114
4.5.2 Effect on frequency and RF power with magnetic field.....	115
4.5.3 Effect on RF output power and frequency with Drift section-II	115
4.6 Conclusion.....	116
CHAPTER 5: DESIGN AND SIMULATION INVESTIGATIONS DUAL-BAND (S-AND C-	
BAND) RBWO WITH SECTIONAL SLOW-WAVE STRUCTURES	121
5.1 Introduction	121
5.2 Design of Dual-Band RBWO with Sectional SWS's	123
5.2.1 Sectional Slow-Wave Structures (SWS-I and -II).....	123
5.2.2 Rectangular Resonant Reflector (RR)	125
5.2.3 Drift Section-I.....	127
5.2.4 Drift Section-II	127
5.3 PIC Simulation of Dual Band RBWO	128
5.4 Parametric Analysis and Discussion	132
5.4.1 Effect on frequency generation and RF power by drift section-I and drift	
section-II (L_{dr1} and L_{dr2})	133
5.4.2 Effect on frequency and RF power by DC magnetic field	135
5.4.3 Effect on frequency and RF power by beam voltage	137
5.5 Conclusion.....	138
CHAPTER 6: DESIGN AND SIMULATION INVESTIGATIONS OF DUAL-BAND (S-AND C-	
BAND) RBWO WITH BRAGG REFLECTOR FOR DIRECT GENERATION OF GAUSSIAN	
PULSE.....	143
6.1 Introduction	143
6.2 Design Methodology of Bragg Reflector and Slow-Wave Structure.....	145
6.2.1 Design Methodology of BRAGG Structure	145
6.3 Slow Wave Structure (SWS).....	151
6.3.1 Design Methodology	151
6.3.2 Cold Dispersion Diagram of Slow Wave Structure	154
6.4 Cut-off Neck Reflector and Drift Sections.....	155
6.5 Tapered Waveguide Collector.....	155

6.6 PIC simulation of Dual band RBWO	158
6.7 Parametric Analysis	163
6.7.1 Effect on frequency and average RF output power with magnetic field.	163
6.8 Conclusion	164
CHAPTER 7: CONCLUSION AND FUTURE SCOPE	169
7.1 Conclusion	169
7.2 Limitations of the Present Work and Future Scope.....	169

LIST OF FIGURES

Figure 1.1: Application domain of HPM at a different frequency and Power level [3].	3
Figure 1.2: Block diagram of an HPM system [3].	4
Figure 1.3: Comparison of HPM sources and conventional microwave sources with respect to optimal impedance and voltage [3].	6
Figure 1.4: Generalized block diagram for linear beam microwave tubes.	9
Figure 1.5: 2D Schematic of HPM source relativistic klystron amplifier (RKA).	13
Figure 1.6: 2D Schematic of HPM source relativistic magnetron (RM).	15
Figure 1.7: 2D Schematic of HPM source virtual cathode oscillator (VCO).	17
Figure 1.8: 2D Schematic of HPM source MILO.	19
Figure 1.9: 2D Schematic of HPM source Reltron.	20
Figure 1.10: Schematic of a FEL with planer wiggler.	22
Figure 1.11: All types of Gyro devices [11].	23
Figure 1.12: 2D Schematic of HPM source RBWO.	25
Figure 1.13: Domains and trends of HPM DEW and EWF [6].	28
Figure 2.1: Schematic of RBWO with overmoded SWS and TRR.	45
Figure 2.2: Working principle for sustained oscillation.	46
Figure 2.3: The Brillouin diagram of the slow-Wave Structure.	48
Figure 2.4: Schematic of cut-off neck reflector.	51
Figure 2.5: Schematic of Cavity RR.	54
Figure 2.6: Schematic of Trapezoidal RR (TRR).	54
Figure 2.7: 2D Schematic of sinusoidal rippled wall SWS. of the sinusoidally corrugated.	57
Figure 2.8: 2D Schematic of a tapered collector.	58
Figure 2.9: A schematic picture of a dispersion relation of TM_{01} mode in infinitely long periodic structure. Two straight lines that intersect the cold structure dispersion curve correspond to Cerenkov and cyclotron beam modes.	58
Figure 2.10: The dependence of beam current on γb .	61
Figure 2.11: The dispersion curve of the beam mode line (1.2 MV) with the TM_{01} mode line.	65
Figure 2.12: Absolute electric field distribution in contour of a cold test, (a) RR and (b) TRR.	67

Figure 2.13: The simulation model of RBWO having an electron beam.....	68
Figure 2.14: RF output powers for the Overmoded RBWO with different reflectors. ..	68
Figure 2.15: (a) Frequency spectrum and (b) The time-frequency of the electric field. 69	
Figure 2.16: Fundamental TM_{01} mode electric field distribution of (a) vector and (b) contour plot.	69
Figure 2.17: Beam voltage depends on (a) RF output power and efficiency and (b) frequency.....	71
Figure 2.18: Influence of developed beam current on RF output power.	71
Figure 2.19: Influence of corrugation amplitude on (a) frequency and (b) RF output power with different periods.	72
Figure 2.20: RF output power and frequency w.r.t drift length.	72
Figure 2.21: RF output power and frequency w.r.t magnetic field.	73
Figure 3.1: 2D Model simulation structure of non-overmoded RBWO ($D/\lambda \approx 1.17$) with RR under guiding magnetic field ~ 0.22 T and DC input voltage 550 kV.	83
Figure 3.2: RF output power versus magnetic field for non-overmoded RBWO ($D/\lambda \approx 1.17$) for the DC input voltage 550 kV. The cyclotron resonances magnetic fields are found at $B_1 \approx 0.10$ T and $B_2 \approx 0.57$ T.	83
Figure 3.3: (a) RF output power and (b) FFT of the RF output signal of non-overmoded RBWO ($D/\lambda \approx 1.52$) with RR under guiding magnetic field of ~ 0.22 T.	84
Figure 3.4: RF output power versus magnetic field for overmoded RBWO ($D/\lambda \approx 1.52$) for the DC input voltage 550 kV. The cyclotron resonances magnetic fields are found at $B_1 \approx 0.07$ T and $B_2 \approx 0.49$ T.	86
Figure 3.5: 2D The Schematic of Trapezoidal Resonant Reflector (TRR).....	86
Figure 3.6: Dispersion curve for (a) non-overmoded RBWO and (b) overmoded RBWO showing TM_{01} mode line and beam mode line intersecting at ~ 3.7 GHz.	86
Figure 3.7: (a) Developed electron beam current ~ 5.9 kA, and (b) DC beam power (voltage*current) ~ 3.25 GW when the applied beam voltage is 550 kV.	87
Figure 3.8: Phase space plot of traversed electrons (at the end of SWS) in radial momentum at ~ 100 ns in (a) non-overmoded RBWO ($D/\lambda \approx 1.17$) with RR at $B = \sim 0.22$ T, (b) non-overmoded RBWO with TRR $B = \sim 0.22$ T, (c) overmoded RBWO ($D/\lambda \approx 1.52$) with RR at $B = \sim 0.19$ T, and (d) overmoded RBWO with TRR at $B = \sim 0.19$ T.	88
Figure 3.9: Phase space plot distribution showing combined influences of SEE (yellow color), HEE (blue color), PCHI (green color) at ~ 100 ns in (a) non-overmoded RBWO ($D/\lambda \approx 1.17$) with RR at $B = \sim 0.22$ T, (b) non-overmoded RBWO with TRR at $B = \sim 0.22$	

T, (c) overmoded RBWO with ($D/\lambda \approx 1.52$) RR at $B = \sim 0.19$ T, and (d) overmoded RBWO with TRR at $B = \sim 0.19$ T.	89
Figure 3.10: Variation of temperature at the collector conducting wall w.r.t to time for (a) non-overmoded SWS, and (b) overmoded SWS.....	91
Figure 3.11: Contour plot of the RF electric field at ~ 100 ns in non-overmoded RBWO ($D/\lambda \approx 1.17$) with RR under the guiding magnetic field ~ 0.22 T.	93
Figure 3.12: Contour plot of the RF electric field at ~ 100 ns in non-overmoded RBWO ($D/\lambda \approx 1.17$) with TRR under the guiding magnetic field ~ 0.22 T.	93
Figure 3.13: Contour plot of the RF electric field at ~ 100 ns in an overmoded RBWO ($D/\lambda \approx 1.52$) with RR under the guiding magnetic field ~ 0.19 T.	93
Figure 3.14: Contour plot of the RF electric field at ~ 100 ns in an overmoded RBWO ($D/\lambda \approx 1.52$) with TRR under the guiding magnetic field ~ 0.19 T.	94
Figure 3.15: RF output power for all four configurations of RBWOs after including the combined causes of pulse shortening.....	94
Figure 4.1: 2D Model of Dual-Band RBWO using Bragg Structure.	105
Figure 4.2: (a) 2D longitudinal cut view of Sectional Bragg Structure.	106
Figure 4.3: Reflection or conversion coefficient vs number of Bragg axial periods... ..	108
Figure 4.4: Dispersion diagram of Sectional Bragg reflector.....	109
Figure 4.5: Dispersion Diagram of Bragg Structure.....	110
Figure 4.6: 2D simulation configuration of the RBWO with sectional Bragg reflector and intense relativistic electron beam particles.	111
Figure 4.7: (a) DC beam voltage (550 kV) and (b) Developed electron beam current (~ 4.66 kA).....	112
Figure 4.8: Instantaneous and average RF output power of the dual-band RBWO with sectional SWS's.	112
Figure 4.9: FFT of the generated HPM wave for RBWO with Sectional Bragg reflector.	113
Figure 4.10: Time-Frequency plot showing generation of frequency.	113
Figure 4.11: Contour plots for the generated mode for both bands at two different time instants.	113
Figure 4.12: Effect of guiding magnetic field on RF power and frequency.....	114
Figure 4.13: Effect of beam voltage on RF power.	115
Figure 4.14: Effect of drift section length (L_{dr2}) on RF output power, and frequency.	115

Figure 5.1: 2D simulation configuration of the dual-band RBWO with sectional SWS and intense relativistic electron beam particles.....	125
Figure 5.2: Dispersion curve of TM_{01} mode and beam mode line of (a) SWS-I and (b) SWS-II.....	125
Figure 5.3: CST cold simulation model of the present dual-band RBWO	126
Figure 5.4: Reflection and transmission coefficients of (a) both RR and drift section-II are present, and (b) only drift section-II is present.	126
Figure 5.5: a) Applied beam voltage in b/w anode and cathode, and b) Developed beam current at the entrance of SWS-I of the present dual-band RBWO.	129
Figure 5.6: Instantaneous and average RF output power of the dual-band RBWO with sectional SWS's.....	129
Figure 5.7: Dual-band axial electric field variation vs time at the end of the simulation.	129
Figure 5.8: The Frequency spectrum of dual-band RBWO with sectional SWS's.....	130
Figure 5.9: Phase-space distribution of electron energy along the axial direction of sectional SWS's at (a) ~6 ns, (b) ~9.8 ns, (c) ~50 ns, and (d) ~100 ns of simulation time (SWS-I region from 250 mm to 500 mm, and SWS-II region from 520 mm to 700 mm).	131
Figure 5.10: Time-frequency spectrogram of the axial electric field (Fig. 5.7).....	132
Figure 5.11: Distribution of axial E-field in the present dual-band RBWO.	132
Figure 5.12: Effect of drift section-I length on (a) time-frequency spectrogram and (b) RF power.	134
Figure 5.13: Effect of drift section-II length on (a) time-frequency spectrogram and (b) RF power.	135
Figure 5.14: Effect of guiding magnetic field on (a) dual-band frequency generation and (b) RF power.....	136
Figure 5.15: Effect of beam voltage on a) dual-band frequency and (b) RF power. ...	137
Figure 6.1: 2D Model of Dual-Band RBWO using Bragg Structure.....	144
Figure 6.2: (a) 2D longitudinal cut view and (b) 3D model of Bragg Structure.....	146
Figure 6.3: Reflection or conversion coefficient Vs (a) Frequency for different N and (b) number of Bragg axial periods for different corrugation depth (R1).	146
Figure 6.4: (a) 3D View of Bragg reflector, and (b) 3D Cut view of Bragg reflector.	148

Figure 6.5: TM ₀₁ mode converted (reflected) from the end of Bragg reflector to TE ₁₁ mode to the end of Bragg reflector (S ₂ (TE ₁₁),2(TM ₀₁)), and the converted (reflected) TE ₁₁ mode penetration at the beginning of Bragg reflector (S ₁ (TE ₁₁),2(TM ₀₁)).	148
Figure 6.6: TM ₀₁ mode reflected from and to the end of Bragg reflector (S ₂ (TE ₀₁),2(TM ₀₁)), and TM ₀₁ mode penetration at the beginning of Bragg reflector (S ₁ (TE ₀₁),2(TM ₀₁)).	148
Figure 6.7: Mode pattern at the output port after mode conversion/reflection from TM ₀₁ at the output port (port 2), i.e., S ₂ (TE ₁₁),2(TM ₀₁).	149
Figure 6.8: Validation of reflection coefficient Vs number of Bragg axial periods using analytical and simulation techniques.	149
Figure 6.9: Dispersion diagram of Bragg structure.	150
Figure 6.10: 2D Schematic of sinusoidal rippled wall SWS.	151
Figure 6.11: (a) Dependence on beam current I _b on ω and (b) Dependence on beam current I _{scl} on V ₀ for different r _b /r ₀ .	154
Figure 6.12: Dispersion diagram for SWS in C-Band.	155
Figure 6.13: 2D schematic shows cathode, cut-off neck reflector and drift Section-1.	156
Figure 6.14: 2D schematic of drift Section-2 separating Bragg and slow wave structures.	156
Figure 6.15: 2D schematic of tapered collector section.	156
Figure 6.16: 2D Model simulation structure of Dual-band RBWO with Bragg reflector under guiding magnetic field 2.0 T and DC input voltage 550 kV.	159
Figure 6.17: Developed electron beam current.	159
Figure 6.18: Instantaneous RF output power.	160
Figure 6.19: Average RF output power with DC input voltage 550 kV.	160
Figure 6.20: FFT of the generated HPM wave for dual-band frequency.	161
Figure 6.21: Particle energy distribution with the function of axial direction at different instances of time.	162
Figure 6.22: Time-Frequency plot showing generation of dual-band frequencies.	162
Figure 6.23: Contour plots of the radial electric field showing linearly polarized TE ₁₁ generated mode shown at a different simulation time.	163
Figure 6.24: Effect of guiding magnetic field on (a) Dual-band frequency generation and (b) RF power.	164

LIST OF TABLES

Table 1.1: Classifications of HPM Sources	7
Table 1.2: Comparison of various experimentally tested HPM Sources	27
Table 2.1: Design Parameters of an S-band RBWO	66
Table 2.2: Comparison of proposed work with previous works.....	70
Table 3.1: Design Parameters for the four configurations of RBWOs.....	84
Table 3.2: Output parameters of all four configurations of RBWOs after Pulse shortening Analysis.....	97
Table 4.1: Design Parameters of Sectional Bragg Reflector.	108
Table 4.2: Design Parameters of SWS.....	110
Table 5.1: Structural Parameters of the Present Dual-Band RBWO.	128
Table 6.1: Optimized Design Parameters of Dual-Band RBWO using Bragg Reflector.	157

LIST OF ABBREVIATIONS

Abbreviation	Full Form
2D	Two Dimensional
3D	Three Dimensional
A	Ampere
AC	Alternating Current
A-K	Anode-Cathode
CRM	Cyclotron Resonant Maser
CARM	Cyclotron Auto-Resonance Maser
CST	Computer Simulation Technology
DC	Direct Current
DEW	Directed Energy Weapon
EEE	Explosive Electron Emission
EM	Electromagnetic
EMP	Electromagnetic Pulse
EWF	Electronic Warfare
FCG	Flux Compression Generator
FDTD	Finite Difference Time Domain
FEM	Finite Element Method
FIT	Finite Integration Technique
FEL	Free Electron Laser
FFT	Fast Fourier Transform
GHZ	Gigahertz
HEE	High Electric field Emission

HFSS	High-frequency Structure Simulator
HPEM	High Power Electromagnetic
HPM	High Power Microwave
Hz	Hertz
IREB	Intense Relativistic Electron Beam
J	Joules
kA	Kilo Ampere
K.E.	Kinetic Energy
kV	Kilo Volt
LINAC	Linear Accelerator
MA	Mega Ampere
MHz	Mega Hertz
MILO	Magnetically Insulated Line Oscillator
MITL	Magnetically Insulated Transmission Line
MPM	Medium Power Microwaves
MW	Megawatt
NRL	Naval Research Laboratory
NS	Nanosecond
PIC	Particle-In-Cell
PCHI	Positively Charged Hydrogen Ions
P.E.	Potential Energy
PFL	Pulse Forming Line
RWO	Relativistic Backward Wave Oscillator
RKA	Relativistic Klystron Amplifier

RKO	Relativistic Klystron Oscillator
RM	Relativistic Magnetron
RF	Radio Frequency
RR	Resonant Reflector
SCO	Split Cavity Oscillator
SEE	Secondary Electron Emission
SSD	Solid-State Devices
SWS	Slow Wave Structure
OSWS	Overmoded Slow Wave Structure
TRR	Trapezoidal Resonant Reflector
TE	Transverse Electric
TM	Transverse Magnetic
TWT	Travelling Wave Tube
UNM	University of New Mexico
μs	Microseconds
VC	Virtual Cathode
VED	Vacuum Electronic Devices
VIRCATOR	Virtual Cathode Oscillator

LIST OF SYMBOLS

Symbol	Details
B	Guiding Magnetic Field
B_1	Cerenkov Absorption
B_2	Cyclotron Absorption
c	Speed of the light
d, P	SWS Period Length
e	Charge of the electron
E	RF electric field
$E_z, E_r, \text{ and } E_\phi$	Axial, Radial, and Azimuthal RF Electric Field
f_r	Resonant frequency
f_c	Cut-off frequency
f	Frequency
I_b	Beam current
I_{st}	Start current
I_{scl}	Space charge limiting current
I_{mn}^J, I_{mn}^Y	Fourier integrals of the Bessel functions of the first and second kind
k	Wavenumber in free space
k_z	Longitudinal wavenumber
K_p	Power reflection coefficient
$L_c, L_{dr}, L_{cut}, L_{dr1}, L_{dr2}$	Cavity/Drift section/Waveguide Length
m	Mass of electron
P_1, P_2, P_3	Axial, Radial, and Azimuthal electron momentum
P_b	Beam Power

r_b	Beam radius
$r_c, r_w, R_c, R_{cut}, R_{dr1}, R_{dr2}$	Cavity/Waveguide Radius
r_0, R_0	Mean Radius
r_1, R_1	Corrugation Depth/Ripple amplitude
s	Resonant Harmonic Number
v_e/v_b	Electron Velocity/Beam Velocity
v_{ph}	Phase Velocity
v_z, v_b	Longitudinal velocity of electron/beam
V	Electrostatic Potential
V_b	Beam Voltage
$z, r, \text{ and } \phi$	Axial, Radial, and Azimuthal axis
θ	Phase
δ	Coupling coefficient
α	Space charge factor
β_o	Normalized beam velocity
γ	Relativistic Factor
γ_0	Initial Relativistic Factor
γ_b	Relativistic Factor under the influence of Space Charge
λ	Wavelength
λ_r	Resonant wavelength
ω	Angular frequency
χ_{mn}	Eigen Value of operating mode

PREFACE

In recent years, the development of High-power microwave (HPM) sources has been very popular in the microwave community due to its various civilian and military applications. The main purpose of HPM sources is to deliberately disrupt or destroy electronic equipment without harming the infrastructure or harming the humans. The generation of RF power by HPM sources from KW's to GW's in the frequency range from GHz to THz with single and dual-frequency by a single HPM device has drawn the attention of researchers and academia around the world for R&D in this domain. There are many HPM sources to generate high power using Relativistic electron beam such as Relativistic Klystron, Relativistic Backward Wave Oscillator (RBWO), Relativistic Magnetron, Magnetically Insulated Line Oscillator (MILO), fast wave devices such as gyro devices and space-charged devices such as Vircator and FEL and these devices are still in active research in many countries. Above all, Relativistic Backward Wave Oscillator (RBWO) is one of the most prominent slow-wave relativistic device used in many applications like E-bomb and Directed Energy Weapons (DEW) applications, and it is more promising HPM source in terms of design, efficiency, repetition rate, and frequency tunability. The only drawback is that it requires a strong external guiding magnetic field. This makes this device cumbersome and can be overcome. Since most applications are used with the help of ground-based stations, I chosen S- and C-bands frequency of operation for my research work.

In the present thesis, the author has designed and simulate the S-band RBWO by considering an experimentally demonstrated S-band overmoded RBWO and the Trapezoidal resonant reflector has been replaced with resonant reflector to enhances the pre-modulation during electron beam propagation, thus increasing the generated RF

signal overall efficiency and coherency. In addition, the pulse shortening study is analyzed by considering its various mechanisms in MAGIC-PIC simulations. Authors tried to develop the look-alike environment causing RF breakdown which leads to the pulse shortening of RF wave. Further, significant use of the helically corrugated cylindrical waveguide named Bragg structure is made to directly generate the HE_{11} / TE_{11} mode from an RBWO for the Gaussian output. The Bragg structure is used as an integral part of a device that performs many functions, such as reflectors, mode converters, and RF interaction structure. It eliminates the requirement of external mode converter to convert outputted TM_{01} mode to Gaussian-like TE_{11} mode which increases the overall length and reduces the overall efficiency of the RBWO device. A single band and dual-band RBWO device are designed and simulated using Bragg structure to achieve high power conversion efficiency. A dual-band relativistic backward wave oscillator (RBWO) with sectional slow-wave structures (SWSs) also has been designed to generate a long high-power microwave (HPM) pulse at two different frequencies.

The author present work has been partially reported in national and international conferences, as well as in reputed journals, in the IEEE Transactions on Electronic Devices, and in the Defence Science Journal. If it useful in the designing, developing, and experimenting with single and dual frequency RBWO, the author would consider his efforts a success.

CHAPTER 1

INTRODUCTION AND LITERATURE REVIEW

CONTENTS

1.1 Introduction

1.2 Overview of High-Power Microwave Sources

1.3 Overview of different HPM Sources

1.3.1 Relativistic Klystron Amplifier

1.3.2 Relativistic Magnetron (RM)

1.3.3 Virtual Cathode Oscillators (VCO or Vircator)

1.3.4 Magnetically Insulated Line Oscillator (MILO)

1.3.5 Reltron

1.3.6 Free Electron Laser

1.3.7 Relativistic Gyrotron Devices

1.4 Relativistic Backward Wave Oscillator (RBWO)

1.4.1 Advantages of an RBWO

1.4.2 Applications of an RBWO

1.5 Literature Review of an RBWO

1.6 Problem Definition

1.7 Outline of the Thesis

1.8 Conclusion

